2018 European Control Conference (ECC)
June 12-15, 2018. Limassol, Cyprus

Battery aging management for Fully Electric Vehicles

Stefano Sabatini[1] and Matteo Corno[1]

Abstract— **Nowadays lithium-ion batteries are the standard power source for electric transportation applications. Lithium-ion batteries are subject to aging and matching the battery life with the vehicle life is still one of the unresolved challenges limiting the large-scale spreading of electric vehicles. This paper explores the possibility of controlling in closed-loop the aging of the battery: the idea is to control the maximum current requested to the battery and to schedule the charging events in order to mitigate the battery degradation. Limiting the use of the battery means compromising with vehicle performance in terms of maximum accelerations, driving range and charge time. The control objective can be therefore defined in minimizing the battery aging and, at the same time, guarantying satisfactory vehicle performance. In the paper the control problem is formally defined in an optimization framework and an optimal benchmark is obtained for future online battery management strategies.**

I. INTRODUCTION

Tightening emissions regulations and increasing governmental incentives programs are motivating car manufacturer efforts in research and development of clean powertrain solutions such as Hybrid and Fully Electric Vehicles (FEV). The biggest limits to FEVs large-scale spreading are the limited driving range, relatively slow recharge time and high cost compared to traditional fuel based vehicles. The high cost is mostly influenced by the battery pack and its replacement during the lifetime of the vehicle: an unresolved challenge is to match the life time of the battery with the life of the vehicle. Lithium-ion batteries are the most common type of batteries for transportation applications due to their exceptional high energy density but, as all other battery chemistries, they are subject to aging. Many different and complex aging mechanisms can be identified in the battery during its lifetime span but macroscopic effects of battery aging are the loss of total storage capacity and the increase of the internal resistance, see [1]. in general battery aging can be divided in two main categories: calendar aging and cycle aging. Calendar aging is associated to the energy storage and it occurs even if the vehicle is not utilized. On the other hand, cycle aging is related to battery utilization (battery charge and discharge) and it strongly depends on how the battery is used. Due to the complexities of the electrochemical phenomena involved in the aging process, most of the studies regarding battery cycle aging are empirical studies [2]–[5]. In these works, battery cells are continuously cycled under different conditions and semi-empirical models are derived from the collected data relating battery loss of capacity to various stress factors like temperature, voltage, SOC and current. It is well established that temperature, Depth of Discharge (DOD), and C-rate are the main stress factors for Lithium-ion batteries. This means that cycling a cell at high C-rate, high temperature and at high DOD makes the cell degrade faster. There are some attempts in controlling the battery aging in Hybrid vehicles: in [6] and [7] the power split between the internal combustion engine (ICE) and the electric motor is decided not only with the objective of minimizing the fuel consumption but battery aging is also taken into account. In this framewotk, the ICE is run in situations where the battery ages faster like high temperature and extreme SOC scenarios. There are some fully electric hybrid configurations where the battery is used jointly to a super capacitor (SC). This solution can be effective to mitigate battery aging since the SC can be used to reduce the battery peak current. The control of such hybrid systems is presented in [8] and in [9]. Up to now, this promising hybrid solution consisting of a battery ad a SC is not as cost effective as over sizing the battery therefore it is rarely used in current FEV.

In this paper, the idea of controlling in closed-loop the capacity loss of a FEV battery is explored. Given that a measure of the reaming battery capacity is available, two control actions can be identified in this sense: 1) setting the maximum admissible current I_{max} that can be drawn from the battery in order to dampen the current peaks 2) limit extreme battery DOD, acting on the vehicle charging management. Ideally, one would like to minimize the capacity degradation but this objective is in contrast with some desired performance of the vehicle in terms of accelerations, driving range and charge time. Therefore, the control objective can be defined as controlling the capacity degradation during the vehicle use and, at the same time, guaranteeing acceptable vehicle performance. One contribution of this paper consists in the development of control-oriented FEV model that can be used to understand and quantify the trade-off existing between limiting the battery usage in terms of maximum current I_{max} and DOD and the vehicle performance. The battery thermal management is also included in the model. Furthermore, an offline optimization procedure of the control variables is carried out to get some insights of the aforementioned trade-off and to set-up an optimal benchmark for future implementation of online control strategies.

The paper is organized as follows: in Section II the FEV model is derived: it consists of the longitudinal vehicle dynamics model, battery model, including its aging submodel, and the cooling system model. Section III shows simulation results exemplifying the effect of the control

[1]Dipartimento Elettronica Informazione e Bioingegneria, Politecnico di Milano , via Ponzio 34/5, 20133, Milano, Italy. (stefano.sabatini, matteo.corno, @polimi.it

variables. In Section IV, an optimization procedure is used to visualize the Pareto-front describing the aforementioned trade-off.

II. Modeling

The objective of this section is to derive a complete vehicle model able to quantify the effect of different driving situations on battery aging. More specifically, the model should be able to provide some insights on the existing trade-off between an optimal usage of the battery (from the point of view of maximizing its lifetime) and some performance indexes such as driving range, charging time and accelerations performance that will be formally defined later on in Section IV. Because of the great amount of data published in literature, the vehicle chosen as a reference is a Nissan Leaf. Relevant data of the vehicle are taken from [10]. The high-level scheme of the developed model is depicted in Figure 1. Three main sub-models can be identified: the vehicle model describing the longitudinal dynamics and the powertrain of the vehicle, the battery cell model that describes the capacity loss of the battery cell depending on the driving conditions and the thermal management module that calculates the power requested to cool down the battery. In the following the three sub-models are described in details.

A. Electric Vehicle model

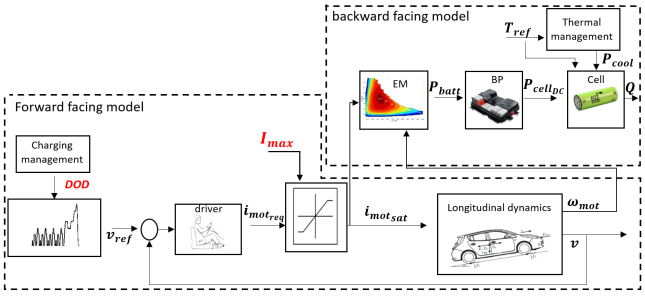

Fig. 1. Scheme of the developed fully electric vehicle model.

The majority of the works regarding powertrain sizing and energy management utilize a backward-facing approach to model the vehicle. In backward approaches, the desired speed is imposed to the vehicle and the motor speed, torque and power are calculated backwards. Differently from this classical approach, the model developed in this work is characterized by a mixed forward-backward facing approach as highlited in Figure 1. The forward-facing part consists in the modeling of the driver's response to a desired speed reference and in the modeling of the longitudinal dynamics of the vehicle. The backward-facing part, based on the power requested to run the vehicle, computes in a backward manner the power that is drawn from the battery. Such an approach turned out to be necessary in the framework used in this paper since the basic assumption that the vehicle is able to meet the speed profile of the driving cycle does not hold. The reader is referred to [11] for more details on forward-facing and backward-facing vehicle simulations.

The model of the driver is a simple PI regulator that requests a certain torque to the electric motor based on the speed error $e = v_{ref} - v$. Knowing the motor torque constant k_t, The motor current can be directly derived from the torque as $i_{req} = \tau_{req}/k_t$. The requested motor current is then saturated to a maximum value I_{max} that, is considered as a control variable to limit the battery current at the cost of limiting also the vehicle acceleration. The motor current is then used to calculate vehicle speed according to the longitudinal vehicle dynamic equation:

$$M\dot{v} = i_{mot_{sat}} \frac{K_t K_g}{R_w} - \frac{1}{2}\rho v^2 C_D A - F_{roll} \tag{1}$$

where K_g is the gear ratio, R_w is the wheel radius, F_{roll} is the rolling resistance, C_D and A are the drag force coefficient and the cross sectional area respectively.

The power that the electric motor has to provide can be calculated from torque and speed:

$$P_{mot} = \frac{K_t i_{mot_{sat}} v}{R_w K_g}. \tag{2}$$

In a backward facing approach, the motor is modeled as a simple efficiency map depending on torque and speed, therefore the power requested to the battery to perform the driving cycle can be calculated dividing the motor power by the motor efficiency:

$$P_{batt_{DC}} = \frac{P_{mot}}{\eta_{mot}(K_t i_{mot_{sat}}, \omega_{mot})}. \tag{3}$$

The power requested to the battery needs to be scaled down to the single cell based on the number of cells present in the battery pack. The battery cell considered in this work is a commercial A123 cylindrical LiFePO4 cell characterized by a nominal voltage of 3.3 V and a nominal capacity of 2.5 Ah. This particular cell has been chosen as reference because it is very well studied in literature, nethertheless the modelling approach used here is general and, if accordingly parametrized, can be applied to any other Li-ion cell. In order to match the voltage and total energy of the Nissan Leaf battery pack, 2910 A123 cylindrical cells need to be used. The cell power is calculate as $P_{cell_{DC}} = P_{batt_{DC}}/n_{cell}$ where n_{cell} is the total number of cells. The DOD of the battery is controlled through the charging management module: when the control schedule a charging event, the charging management block modifies the driving cycle in order to stop the vehicle and perform the charging of the battery.

B. Battery cell model

Inputs to the cell model are the requested power to the cell P_{cell} and the operating temperature T. The cell is modeled using an electrical equivalent circuit characterized by a voltage source V_{OC} and its internal resistance R. The open circuit voltage depends on the state of charge through the well known OCV curve, while the internal resistance is a function of the aging of the battery and of the operating temperature. The parameters of the equivalent circuit are

taken from [12]. With a simple power balance the cell current can be obtained as a function of the requested power:

$$I = \frac{V_{OC} - \sqrt{V_{OC}^2 - 4RP_{cell}}}{2R}. \quad (4)$$

The State of Charge SOC is computed as the integral of the current flowing into the cell normalized by the actual capacity of the cell Q that, as already mentioned, is aging dependent.The aging model is inspired by the one experimentally identified in [2] on the same A123 cell described above. It is formulated here as a nonlinear differential equation describing the rate of capacity loss with respect to the Ah processed:

$$\begin{aligned} \frac{dQ}{dAh} &= -\frac{z}{100}\alpha_{SOC}\exp\left(\frac{-E_a+\eta I_c}{R_g(273.15+T)}\right)Ah^{z-1} \\ \frac{dAh}{dt} &= \frac{1}{3600}|I_c Q_{nom}| \end{aligned} \quad (5)$$

where the second differential equation simply defines the Ah throughput as the total amount of current processed by the cell. According to (5), three main stress factors influence the battery degradation: cell temperature T, C-Rate I_c defined as the operating current normalized by the nominal cell capacity Q_{nom}, and SOC. Regarding the effect of temperatue and C-Rate, the aging model described here is in line with [2] and other scentific works (e.g. [4], [3]) according to which, for the same amount of charge processed, cycling a battery at high temperature or at high C-Rate makes the internal aging processes faster leading to a bigger loss of capacity. Regarding the effect of SOC, the results presented in [2] showed a very low (almost negligible) effect of the SOC on aging. This result can be explained by the fact that the considered range of SOC was limited to $30\% - 75\%$ that is the reasonable operating range for a Hybrid electric vehicle where the supervisory control runs the internal combustion engine at very low and very high SOC. In the case of FEVs, it is important to account for the effect of high and low SOC on battery aging in case the driver wants to exploit the full capacity of the battery to extend the range of the vehicle. Previous works such as [5] and [13] showed that substantial depths of discharge that lead the battery to operate below 20% and above 80 % of SOC affect the battery aging. For this reason the aging model (5) includes the penalizing factor α_{SOC} in order to provide a faster aging rate at high and low state of charge. The coefficient α_{SOC} is defined as follows:

$$\alpha_{SOC} = (1 + ce^{b(SOC_{min} - SOC)})(1 + ce^{b(SOC - SOC_{max})}) \quad (6)$$

where c, b, SOC_{min} and SOC_{max} are tuning parameters that can be used to shape the penalization function and that, in practice, should be identified through ad-hoc aging experiments. Figure 2 shows the parametrization of α_{SOC} chosen in this work.

Beside the loss of capacity, battery aging results in an increase of the internal resistance R. Inspired by the experimental results published in [14] a linear relationship between resistance increment ΔR and capacity decrement ΔQ is assumed.

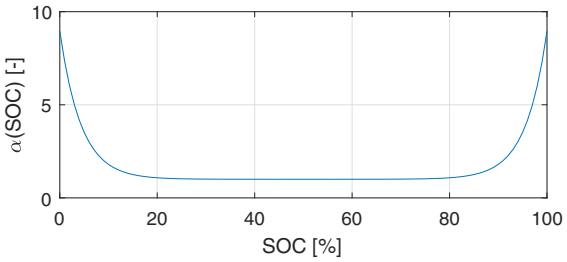

Fig. 2. Chosen parametrization of α_{SOC} used to penalize low and high SOC.

C. Thermal management

As discussed in Section II-B, temperature is an important factor for battery aging since high temperatures accelerate the aging process. This fact motivated most of the electric car makers to include a battery cooling system in their battery pack design. The model developed here includes the effect of a cooling system that has the task of keeping the temperature of the cell to a constant reference value T_{ref}. The simplified scheme of the cooling system is represented in Figure 3.

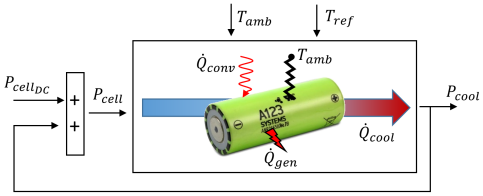

Fig. 3. scheme of the cooling system model.

In a steady state condition, the cooling system has to remove the heat generated inside the cell plus the convective heat from the ambient:

$$\begin{aligned} \dot{Q}_{cool} &= \dot{Q}_{gen} + \dot{Q}_{conv} \\ \dot{Q}_{gen} &= RI_{cell}^2 \\ \dot{Q}_{conv} &= (T_{amb} - T_{ref})/R_{conv} \end{aligned} \quad (7)$$

where R_{conv} is the thermal resistance from the cell to the ambient. The electric power consumed by the cooling system P_{cool} depends on the rate of the heat removed divided by the Coefficient of Performance COP of the cooling system. The COP depends on the ambient temperature since it becomes less efficient to remove heat as the external temperature increases. A reasonable COP function is taken from [15]. The electric power from the cooling system is then summed to the power requested by the driving cycle. In this manner the effect of the temperature control of the cell translates into an additional power load, hence an additional current, requested to the cell itself.

III. Simulation results

It is difficult to validate a battery aging model on real vehicle data because an ad hoc experimental campaign is very costly and time consuming. In order to give a rough idea of the model validity, the capacity degradation calculated by the proposed model is compared with some experimental data published online. Despite the great amount of vehicle parameters published online for the Nissan Leaf, no clear experimental analysis has been found regarding its battery aging. Therefore the capacity loss predicted by the proposed model has been compared with experimental data publsihed in [16] for the Tesla Model S. The model is run over a mixed urban-highway Artemis cycle at a constant temperature of 30 degrees Celsius. Figure 4 shows how the capacity calculated by the model reproduce reasonably well the capacity loss of the Tesla battery. This comparison should be intended as a reasonableness check other than a rigorous model validation.

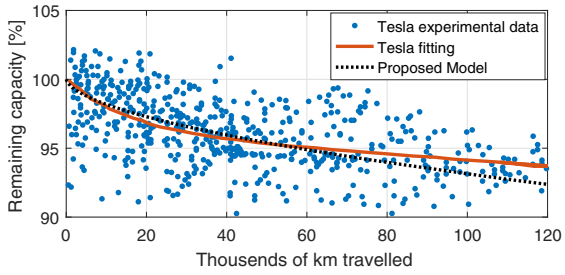

Fig. 4. Model capacity degradation simulated over a mixed urban-highway Artemis cycle compared to Tesla Model S experimental Data. Figure reproduced from [16].

In the following, some simulations results are presented to demonstrate the the effect of the control variables I_{max} and DOD on battery capacity loss and vehicle performance. In first approximation, it is possible to relate the maximum motor current to the maximum allowable cell current through the following power balance:

$$I_{max} = \frac{I_{max_{cell}} V_{cell_{nom}} n_{cell}}{\omega_{mot} K_t \bar{\eta}} \tag{8}$$

where $\bar{\eta}$ is an average electric motor efficiency. Therefore, in the following, the maximum allowable cell current $I_{max_{cell}}$ is considered as a control variable that can be translated in a maximum motor current through the approximated relation described by (8). Figure 5 shows the effect of limiting the maximum current drained from the battery during a simulation where the electric vehicle performed the US Federal Test Procedure (FTP cycle) for a total distance of 30000 km.

The result is that, for the same traveled distance, limiting the maximum current at 0.75 C helps in limiting the loss of battery capacity: at 30000 km there is a 0.25% of capacity saved that corresponds to an improvment of 10% with respect to the nominal case without current limitation. There is a price to pay in controlling the maximum current: limiting the maximum current means limiting the maximum acceleration

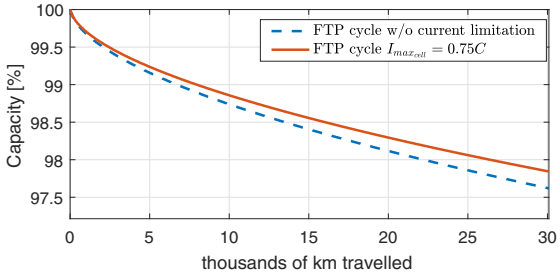

Fig. 5. Effect of current limitation on cell capacity, DOD fixed to 60%.

during driving and slows down the charging process. Figure 6 shows the actual speed profile of the vehicle compared with the FTP reference speed: It is clear how, limiting the current, the vehicle is not able to follow the reference during demanding accelerations especially at high speeds. It is important to remark that the effect of limiting the maximum current on cell capacity is strictly dependent on the driving cycle: for the same maximum limit $I_{max_{cell}}$, if the speed profile is very demanding in terms of accelerations, the benefit on the capacity will be relevant. In case the speed profile is so smooth that the current request rarely exceeds the limit, the effect will be almost negligible.

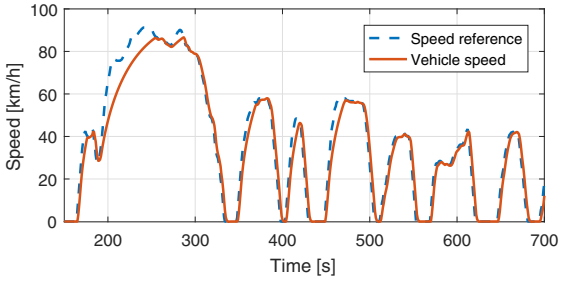

Fig. 6. Effect of current limitation on speed reference tracking.

Figure 7 shows the effect of DOD on cell capacity. It can be seen that reducing the DOD down to 60% can save 1% of battery capacity in the first 30000 km. The price to pay in this case is that the range is substantially reduced because 40% of the capacity of the battery is not exploited at all. As a side effect, the charging time is reduced.

In the considered situation, it can be noted that limiting the DOD has a more evident effect on battery aging compared to setting a limit on the maximum current: this fact is a peculiarity of FEV compared to hybrid vehicles. In hybrid powertrains, the battery size is much smaller since it does not have to guarantee a long driving range but the battery is subject to higher currents in order to power the entire vehicle in EV mode. Furthermore DOD usually has a small influence in hybrid vehicles because the supervisory controller never runs the battery at extreme SOC values. On the other hand FEV are designed with large battery packs resulting in smaller cell currents and therefore a smaller current sensitivity on battery degradation.

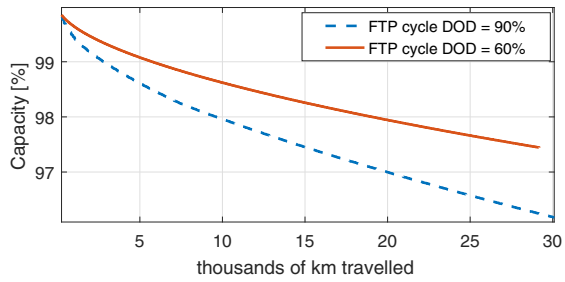

Fig. 7. Effect of DOD on cell capacity with no maximum current limitation.

IV. Optimization Framework

It is now clear that there are several trade-offs to be taken into account if we want to manage the battery degradation in FEV. It is therefore interesting to further analyze the trade-off in an offline optimization framework. This is also useful in order to create an optimal benchmark for online control strategies. To do so, we can define 4 indexes of performance: J_{life}, J_{speed}, J_{charge}, J_{range}. Considering an optimization horizon $[0, t_{end}]$, we can define J_{life} as the capacity degradation over the considered time horizon normalized by the traveled kilometers:

$$J_{life} = \frac{Q(0) - Q(t_{end})}{\Delta km}. \tag{9}$$

J_{speed} is defined as the root mean square value of the speed difference between the cycle reference and the actual speed of the vehicle:

$$J_{speed} = \sqrt{\frac{1}{t_{end}} \int_0^{t_{end}} (v_{ref}(\tau) - v(\tau))^2 d\tau}. \tag{10}$$

This index represents the driveability of the vehicle. J_{charge} and J_{range} are the root mean square values of the charge time and driving range calculated over the charging events in the considered time horizon:

$$\begin{aligned} J_{charge} &= \sqrt{\frac{1}{N} \sum_{i=1}^{N} t_{charge(i)}^2} \\ J_{range} &= \sqrt{\frac{1}{N} \sum_{i=1}^{N} range^2(i)} \end{aligned} \tag{11}$$

where N is the total number of charging events performed in the horizon. During the vehicle life, ideally one would like to minimize the battery aging J_{life} and the charge time J_{charge}, maximize the driving range J_{range} and to perfectly follow the speed reference *i.e.* minimizing J_{speed}. Of course this objective functions are in contrast with each other and more specifically, the minimization of J_{life} is in contrast with the other terms. The multi-objective optimization problem can be reduced to a single-objective optimization problem that consists in finding the optimal control variables DOD, $I_{max_{cell}}$ to minimize a weighted summation of the various terms:

$$\begin{aligned} &\min_{DOD, I_{max}} \; J_{tot} \\ &J_{tot} = \alpha_l J_{life} + \alpha_c J_{charge} - \alpha_r J_{range} + \alpha_s J_{speed}. \end{aligned} \tag{12}$$

Depending on the weights α_l, α_c, α_r, α_s one can give more importance to one or more aspects of the problem over the others. The objective of this preliminary study is to quantify the trade off between battery aging and the performance of the vehicle, therefore α_c, α_r, α_s are chosen to make J_{speed}, J_{range} and J_{charge} have the same weights in the cost function, while the optimization has been performed several times with different values of α_l. A total horizon of 30000 km of the FTP cycle and a control horizon of 3000 km have been chosen for the optimization. In practice, in each control horizon, $I_{max_{cell}}$ and DOD are found to minimize the overall cost function (12). A Particle Swarm Optimization (PSO) has been used to solve the series of optimization problems using a swarm size of 200 particles. The results of the optimization for different values of α_l are summarized in Figure 8.

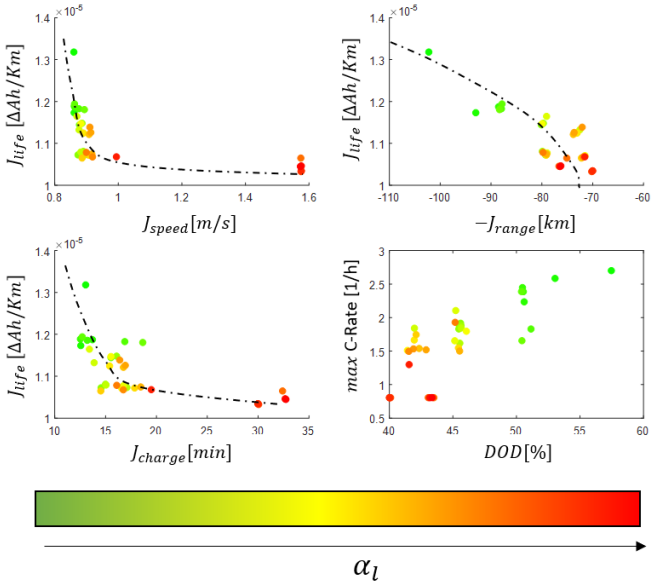

Fig. 8. Pareto-front like representation of the battery life vs vehicle performance.

The first three plots represent the trade-off between J_{life} and the other performance indexes, the forth plot represents the mean values of the optimal control variables over the entire horizon. For low-medium values of α_l (green and yellow dots), the optimal control action mainly results in reducing the DOD with a consequent reduction of the driving range. For this range of α_l, $I_{max_{cell}}$ is also reduced from 3C to 2C causing a slow down of the average charge time. Driveability is not affected in this range since J_{life} is reduced without affecting J_{speed}: this is due to the fact that the FTP cycle never demands for long periods of time battery currents over 2C, therefore the accelerations performance of the vehicle are not modified. As we increase the weight on battery aging (red dots), the control action results in reducing the maximum

current below 1C and in a consequent deterioration of the acceleration performance (J_{speed}). Furthermore, the optimal control variables for a value of α_l located at the 'elbow' of the Pareto curve (yellow-orange dots) are computed over an horizon of 200000 km, a value that usually approaches the vehicle useful life. The control variables along with the capacity loss are plotted in the time domain in Figure 9. As it can be seen, larger control efforts are used in the first 50 thousands kilometers: DOD is limited below 50 % and the cell current is limited below 2C. After the first 50 thousands kilometers, the optimal DOD and $I_{max_{cell}}$ settle around a constant value of 50% and 2.5 C respectively. This behavior is due to the fact that the aging degradation rate is higher for the first thousands Ah processed by the battery, motivating a greater control effort in the first thousands kilometers compared to the rest of the vehicle life. The capacity plot in Figure 9 shows how the optimal control sequence performs compared to using constant DOD and I_{max} over the entire vehicle life. A very limited DOD and I_{max} (es: 40% and 1.5 C respectively) produces the highest remaining capacity but strongly limit the range and the other vehicle performance for the whole vehicle life span. More relaxed constraints on DOD and I_{max} (es: 50% and 2.5 C respectively) allows better performance but results in a higher capacity degradation. The optimal control sequence stands in the middle: it limits the battery stress in the first part of the vehicle life and then reduces the control effort after 50000 kilometers.

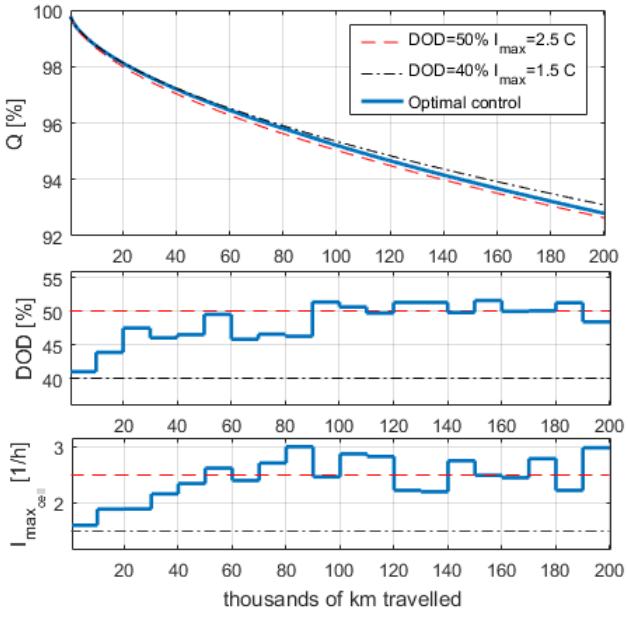

Fig. 9. Time history of the optimal control variables $I_{max_{cell}}$ and DOD.

V. CONCLUSIONS

In this paper, the problem of controlling in closed-loop the battery aging of a FEV has been defined. An ad-hoc electric vehicle model has been developed for this specific purpose. Furthermore, the existing trade-off between limiting battery usage in order to mitigate its degradation and vehicle performances has been explored in an optimization framework. The offline optimization framework gives us a benchmark that poses the basis for future implementations of online aging management strategies. The result presented here are relative to a specific driving cycle (FTP), future work will also focus on analyzing the sensitivity of the optimal control solution to different driving cycles.

ACKNOWLEDGMENT

This work was supported by MIUR SIR project RBSI14STHV.

REFERENCES

[1] A. Barré, B. Deguilhem, S. Grolleau, M. Gérard, F. Suard, and D. Riu, "A review on lithium-ion battery ageing mechanisms and estimations for automotive applications," *Journal of Power Sources*, vol. 241, pp. 680–689, 2013.

[2] G. Suri and S. Onori, "A control-oriented cycle-life model for hybrid electric vehicle lithium-ion batteries," *Energy*, vol. 96, pp. 644–653, 2016.

[3] I. Baghdadi, O. Briat, J.-Y. Delétage, P. Gyan, and J.-M. Vinassa, "Lithium battery aging model based on dakins degradation approach," *Journal of Power Sources*, vol. 325, pp. 273–285, 2016.

[4] J. Wang, P. Liu, J. Hicks-Garner, E. Sherman, S. Soukiazian, M. Verbrugge, H. Tataria, J. Musser, and P. Finamore, "Cycle-life model for graphite-lifepo4 cells," *Journal of Power Sources*, vol. 196, no. 8, pp. 3942–3948, 2011.

[5] M. Ecker, N. Nieto, S. Käbitz, J. Schmalstieg, H. Blanke, A. Warnecke, and D. U. Sauer, "Calendar and cycle life study of li (nimnco) o2-based 18650 lithium-ion batteries," *Journal of Power Sources*, vol. 248, pp. 839–851, 2014.

[6] L. Tang, G. Rizzoni, and S. Onori, "Energy management strategy for hevs including battery life optimization," *IEEE Transactions on Transportation Electrification*, vol. 1, no. 3, pp. 211–222, 2015.

[7] S. Ebbesen, P. Elbert, and L. Guzzella, "Battery state-of-health perceptive energy management for hybrid electric vehicles," *IEEE Transactions on Vehicular technology*, vol. 61, no. 7, pp. 2893–2900, 2012.

[8] R. Carter, A. Cruden, and P. J. Hall, "Optimizing for efficiency or battery life in a battery/supercapacitor electric vehicle," *IEEE Transactions on Vehicular Technology*, vol. 61, no. 4, pp. 1526–1533, 2012.

[9] Z. Song, H. Hofmann, J. Li, X. Han, X. Zhang, and M. Ouyang, "A comparison study of different semi-active hybrid energy storage system topologies for electric vehicles," *Journal of Power Sources*, vol. 274, pp. 400–411, 2015.

[10] J. G. Hayes and K. Davis, "Simplified electric vehicle powertrain model for range and energy consumption based on epa coast-down parameters and test validation by argonne national lab data on the nissan leaf," in *Transportation Electrification Conference and Expo (ITEC), 2014 IEEE*, pp. 1–6, IEEE, 2014.

[11] G. Mohan, F. Assadian, and S. Longo, "Comparative analysis of forward-facing models vs backward-facing models in powertrain component sizing," 2013.

[12] X. Lin, H. E. Perez, S. Mohan, J. B. Siegel, A. G. Stefanopoulou, Y. Ding, and M. P. Castanier, "A lumped-parameter electro-thermal model for cylindrical batteries," *Journal of Power Sources*, vol. 257, pp. 1–11, 2014.

[13] J. Schmalstieg, S. Käbitz, M. Ecker, and D. U. Sauer, "A holistic aging model for li (nimnco) o2 based 18650 lithium-ion batteries," *Journal of Power Sources*, vol. 257, pp. 325–334, 2014.

[14] S. F. Schuster, M. J. Brand, C. Campestrini, M. Gleissenberger, and A. Jossen, "Correlation between capacity and impedance of lithium-ion cells during calendar and cycle life," *Journal of Power Sources*, vol. 305, pp. 191–199, 2016.

[15] T. Malik and C. Bullard, "Air conditioning hybrid electric vehicles while stopped in traffic," tech. rep., Air Conditioning and Refrigeration Center. College of Engineering. University of Illinois at Urbana-Champaign., 2004.

[16] F. Lambert, "Tesla battery data shows path to over 500,000 miles on a single pack," Jan 2016.